

Fluorescence Resonance Energy Transfer Reveals a Binding Site of a Photosensitizer for Photodynamic Therapy¹

Rachel L. Morris, Kashif Azizuddin, Minh Lam, Jeffrey Berlin, Anna-Liisa Nieminen, Malcolm E. Kenney, Anna C. S. Samia, Clemens Burda, and Nancy L. Oleinick²

Departments of Radiation Oncology [R. L. M., K. A., N. L. O.] and Anatomy [A.-L. N.], School of Medicine; Case Western Reserve University/Ireland Comprehensive Cancer Center [M. L., A.-L. N., M. E. K., N. L. O.]; Department of Chemistry [J. B., M. E. K., A. C. S. S., C. B.]; and the Center for Chemical Dynamics and Nanomaterials Research [A. C. S. S., C. B.], Case Western Reserve University, Cleveland, Ohio 44106

Abstract

Phthalocyanine (Pc) 4, like many photosensitizers for photodynamic therapy (PDT), localizes to intracellular membranes, especially mitochondria. Pc 4-PDT photodamages Bcl-2 and Bcl-xL, antiapoptotic proteins interacting with the permeability transition pore complex that forms at contact sites between the inner and outer mitochondrial membranes. These complexes and the inner membrane are unique in containing the phospholipid cardiolipin. Nonyl-acridine orange (NAO) is a specific probe of cardiolipin. Here we show evidence for fluorescence resonance energy transfer from NAO to Pc 4, defining a binding site for the photosensitizer. This observation establishes an innovative tool for exploring the localization of other photosensitizers and additional fluorescent, mitochondrion-localizing drugs having appropriate spectral properties.

Introduction

PDT,³ a novel cancer therapy, generates singlet oxygen via visible light activation of a photosensitive dye accumulated in the tumor (1). Most photosensitizers are porphyrins, *e.g.*, the first approved photosensitizer Photofrin, or related macrocycles. Pc 4, a second-generation photosensitizer now in clinical trial (2), localizes in mitochondria and the endoplasmic reticulum (3, 4), but it has been difficult to determine the precise binding sites at the molecular level. On the basis of the ability of Pc 4-PDT to photodamage Bcl-2 (5) and Bcl-xL⁴ and the extremely limited range of singlet oxygen in cells (6), it is inferred that Pc 4 binds within a few nanometers of these antiapoptotic proteins. Both Bcl-2 and Bcl-xL interact with the voltage-dependent anion channel (VDAC; Ref. 7), a component of the permeability transition pore that forms at the contact sites between the inner and outer mitochondrial membranes (8). The phospholipid CL is located almost exclusively in the inner mitochondrial membrane and at the mitochondrial contact sites (9). CL is tightly bound to many proteins crucial for mitochondrial function, such as the respiratory complexes, cytochrome *c*, and components of the permeability transition pore (9, 10). The fluorescent dye NAO, a specific probe of CL (11), has been used to image CL by confocal microscopy (12), to measure mitochondrial mass (13), and to quantify CL in the leaflets of the mitochondrial inner membrane (14). NAO and Photofrin may compete for the same binding site on CL in mitochondria (15). A reduced ability of ZnPc to

transfer from liposomes to isolated mitochondria was found if the liposomes contained CL, implying a high affinity of zinc Pc for CL (16). Here, we present direct evidence for the binding of a photosensitizer to sites on CL, based on FRET between NAO and Pc 4. This is a powerful new technique for studying the localization of photosensitizers and other mitochondrion-targeting drugs that are planar aromatic fluorescent species with appropriate spectral properties.

Materials and Methods

Cell Culture. Human prostate cancer PC-3 cells were grown in RPMI 1640 containing 10% fetal bovine serum and penicillin/streptomycin (100 μ g/ml) in 5% CO₂/95% air at 37°C in a humidified incubator.

Reagents. A stock solution (0.5 mM) of the Pc photosensitizer Pc 4 (2) was prepared in DMF and stored in the dark at 4°C. A stock solution (1 mM) of NAO (Molecular Probes, Inc., Eugene, OR) was prepared in methanol.

Confocal Microscopy. PC-3 cells were plated at 2×10^5 cells/dish in 35-mm glass-bottom coverslip dishes, and incubated with Pc 4 (200 nM in complete medium) overnight at 37°C. After removal of the Pc 4-containing medium, 1 ml of serum-free medium containing NAO (200 or 500 nM) and/or Mitotracker Red (75 nM) was added to the dishes for 30 min at 37°C. All of the samples were imaged in 1 ml of phenol red-free HBSS with 5 mM glucose. A 63 \times N.A. 1.4 oil immersion planapochromat objective was used with a Zeiss LSM 510 NLO confocal microscope system (3, 4). Images of NAO fluorescence were collected using 488-nm excitation light from an argon laser and a 500–550-nm band pass-barrier filter. Images of Pc 4 fluorescence were obtained using 633-nm excitation light from the HeNe2 laser and a 650-nm long-pass filter. Images of Mitotracker Red (Molecular Probes) fluorescence were obtained using 543-nm excitation light from the HeNe1 laser and a 560-nm long-pass filter.

Flow Cytometry. PC-3 cells were plated in 60-mm Petri dishes at 5×10^5 cells/dish and were incubated with Pc 4 (200 nM in complete culture medium) overnight at 37°C. After removal of the Pc 4-containing medium, 5 ml of serum-free medium containing NAO (50–500 nM) were added to the dishes for 30 min at 37°C. The medium was removed, and cell monolayers were collected by a brief trypsinization. The cell suspension was centrifuged at $\sim 2250 \times g$ for 5 min, and the pellet was resuspended in 0.5 ml of phenol red-free HBSS. An analysis of NAO and Pc 4 was carried out on an EPICS Elite flow cytometer. Samples were excited at 488 nm, and the fluorescence emission was collected in two wavelength bands: (a) 525 ± 13.5 nm and (b) 675 ± 12.5 nm.

Fluorescence Spectroscopy. PC-3 cells were plated and processed as described for flow cytometry, except that cell pellets were resuspended in 2 ml of phenol red-free HBSS with 5 mM glucose. Absorption and fluorescence were measured in 1-cm path length quartz cuvettes, using a Varian Cary 50 Bio UV-vis and Varian Cary Eclipse fluorescence spectrophotometer. The quantum yield of Pc 4 was determined using zinc(II) tetraphenylporphine ($\phi_{\text{DMF}} = 0.04$) as standard. NAO solutions in DMF or NAO-loaded cells were excited with 488-nm light, and emission was collected between 498 nm and 750 nm. Pc 4 solutions in DMF or Pc 4-loaded cells were excited with 633-nm light and emission collected between 643 nm and 750 nm. Samples containing both NAO and Pc 4 were excited with either 488-nm or 633-nm light.

Received 5/27/03; revised 7/2/03; accepted 7/09/03.

The costs of publication of this article were defrayed in part by the payment of page charges. This article must therefore be hereby marked *advertisement* in accordance with 18 U.S.C. Section 1734 solely to indicate this fact.

¹ Supported by Grants R01 CA83917, P01 CA48735, and P30 CA43703 from the National Cancer Institute, NIH.

² To whom requests for reprints should be addressed, at Department of Radiation Oncology, School of Medicine (BRB-324), Case Western Reserve University, 10900 Euclid Avenue, Cleveland, OH 44106-4942. Phone: (216) 368-1117; Fax: (216) 368-1142; E-mail: nlo@po.cwru.edu.

³ The abbreviations used are: PDT, photodynamic therapy; CL, cardiolipin; DMF, dimethylformamide; FRET, fluorescence resonance energy transfer; NAO, 10-*N*-nonyl-acridine orange; Pc, phthalocyanine(s).

⁴ Xue *et al.*, submitted for publication.

Results and Discussion

The subcellular localization of NAO and Pc 4 in PC-3 cells was determined by confocal microscopy (Fig. 1). No fluorescence was detected when Pc 4 was excited at 488 nm or when NAO was excited with 633-nm of light (data not shown). NAO bound specifically to mitochondria as measured by colocalization with Mitotracker Red (data not shown), and Pc 4 partially colocalized with NAO (Fig. 1B). To determine whether the prior binding of Pc 4 modulates the fluorescence of NAO, PC-3 cells were incubated with 50–500 nM NAO with or without preloading with 200 nM Pc 4. In the flow cytometer, the cells were excited with 488-nm light, and emitted light was collected in two wavelength bands: (a) 525 ± 13.5 nm, the peak of NAO emission; and (b) 675 ± 12.5 nm, the peak of Pc 4 emission. Cells containing only Pc 4 produced no fluorescence when excited by 488-nm light (data not shown). NAO-loaded cells displayed a concentration-dependent increase in emitted fluorescence in both of the wavelength bands, with the 525-nm band emitting about 10-fold more fluorescence than the 675-nm band (Fig. 2 and data not shown). In cells containing both Pc 4 and NAO, there was no large, detectable change in the 525-nm fluorescence, but there was an ~ 2 -fold increase in fluorescence at 675 nm (Fig. 2). The results are consistent with FRET between NAO and Pc 4.

Further evidence of FRET between NAO and Pc 4 was found by spectrofluorometry (Fig. 3). In DMF, there is virtually no overlap between the absorption spectra of the two dyes ($\lambda_{\max} = 495$ nm for NAO and 668 nm for Pc 4; Fig. 3A). The emission spectrum of NAO slightly overlaps the absorption spectrum of Pc 4 within the 550–650-nm region (Fig. 3A). There was no emission at $\lambda > 650$ nm when a DMF solution of NAO and Pc 4 was excited at 488 nm. This result was expected, because both molecules are soluble and solvated in DMF. In a biological milieu, the spectral peaks are slightly broadened (data not shown). Fluorescence ($\lambda_{\max} = 675$ nm) was observed when Pc 4-loaded cells were excited at 633 nm but was not observed at 488 nm (Fig. 3B), and 633-nm light elicited no emission from NAO-loaded cells (data not shown). When cells loaded with NAO were excited at 488 nm, a single emission peak was observed with $\lambda_{\max} \sim 525$ nm and no evidence for a second peak at wavelengths > 600 nm (Fig. 3, B and C). In contrast, when Pc 4-loaded cells were incubated

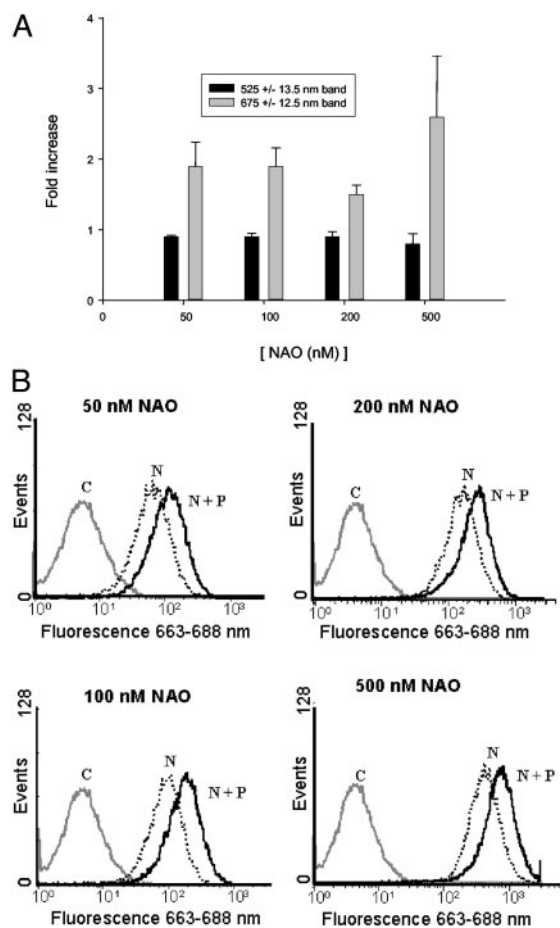


Fig. 2. Fluorescence emission of PC-3 cells containing NAO \pm Pc 4. PC-3 cells were incubated with 0 or 200 nM Pc 4 for 16 h, then with 50–500 nM NAO for 30 min, followed by flow cytometric analysis. Samples were excited by 488-nm light, and the emission was collected in two wavelength bands: (a) 525 ± 13.5 nm and (b) 675 ± 12.5 nm. A, the fold increase in fluorescence in the presence of Pc 4 was calculated as the ratio of the mean channel fluorescence of the NAO + Pc 4 sample to the mean channel fluorescence of the NAO-only sample. The figure represents the mean and SE of five trials. B, histograms for fluorescence in the 675 ± 12.5 nm band from a representative experiment; C, control PC-3 cells; N, cells with NAO only; N + P, cells with NAO + Pc 4.

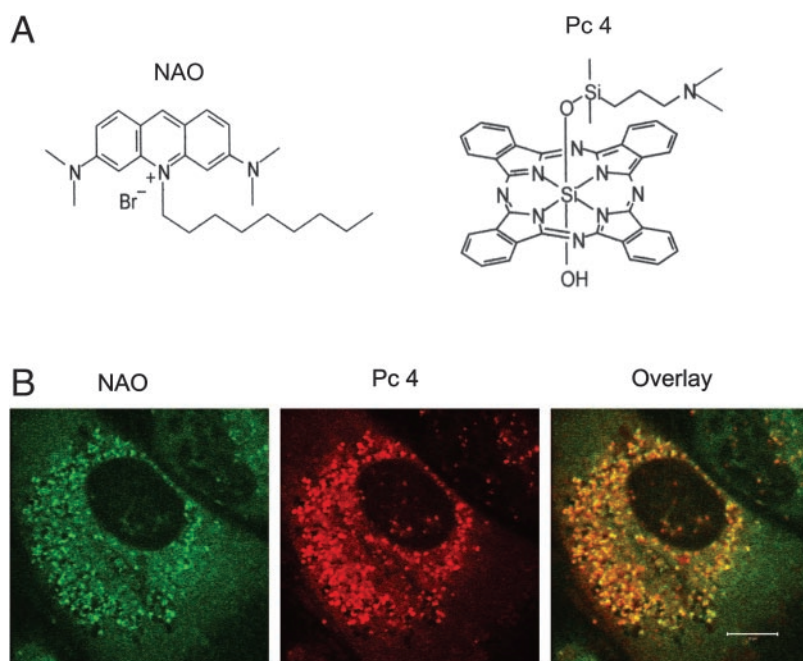


Fig. 1. Structures (A) and colocalization (B) of NAO and Pc 4. For B, PC-3 cells were incubated with 200 nM Pc 4 for 16 h and with 500 nM NAO for 30 min at 37°C. Localization was analyzed by confocal microscopy. Scale bar, 10 μ m.

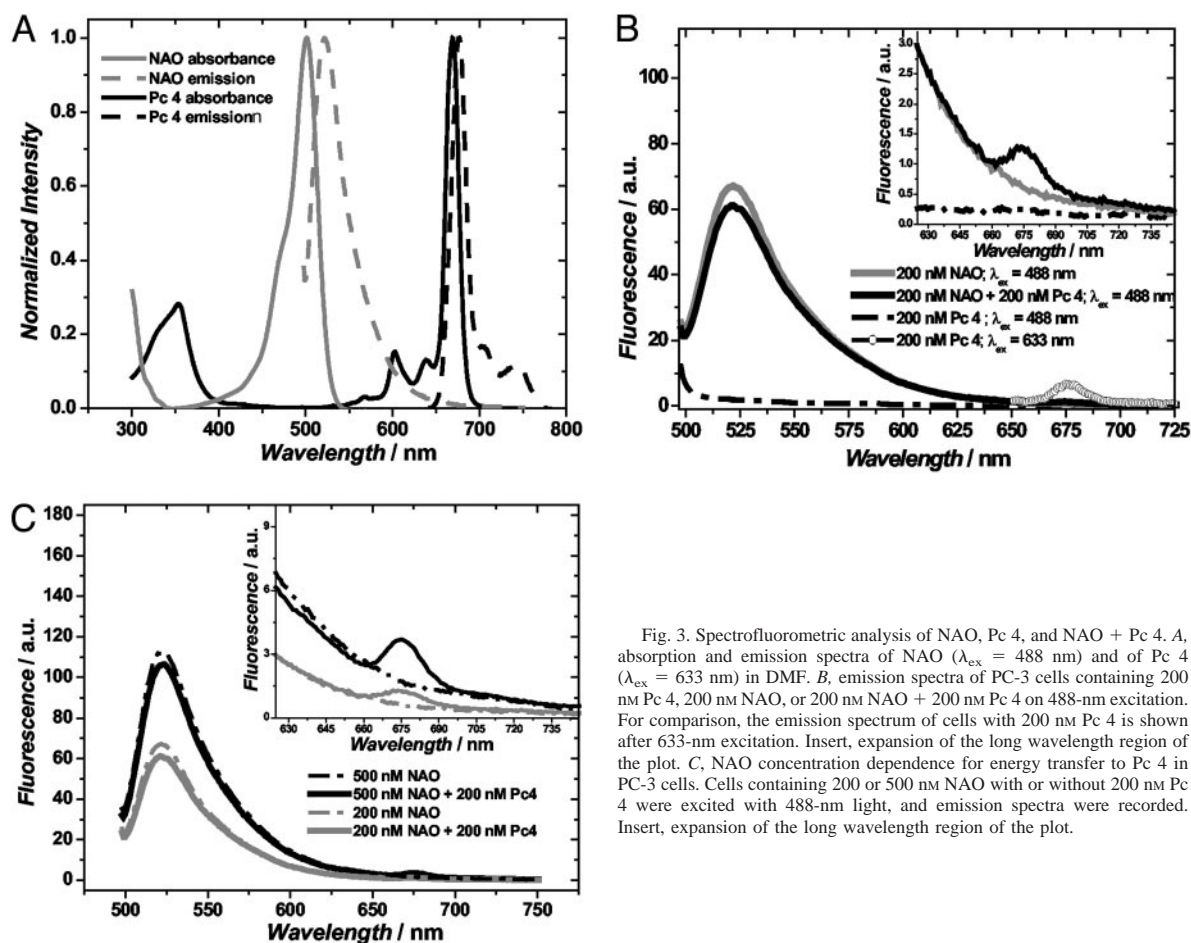


Fig. 3. Spectrofluorometric analysis of NAO, Pc 4, and NAO + Pc 4. A, absorption and emission spectra of NAO ($\lambda_{\text{ex}} = 488$ nm) and of Pc 4 ($\lambda_{\text{ex}} = 633$ nm) in DMF. B, emission spectra of PC-3 cells containing 200 nM Pc 4, 200 nM NAO, or 200 nM NAO + 200 nM Pc 4 on 488-nm excitation. For comparison, the emission spectrum of cells with 200 nM Pc 4 is shown after 633-nm excitation. Insert, expansion of the long wavelength region of the plot. C, NAO concentration dependence for energy transfer to Pc 4 in PC-3 cells. Cells containing 200 or 500 nM NAO with or without 200 nM Pc 4 were excited with 488-nm light, and emission spectra were recorded. Insert, expansion of the long wavelength region of the plot.

with NAO, excitation at 488 nm produced a decrease in the 525-nm emission and a new peak at 675 nm (Fig. 3, B and C). The reduction of the 525-nm emission and the size of the 675-nm emission were greater for 500 nM NAO than for 200 nM NAO (Fig. 3C). In none of the experiments was there evidence for fluorescence consistent with a NAO dimer ($\lambda_{\text{em}} \sim 650$ nm; Ref. 17). Thus, excitation of NAO with 488-nm light resulted in emission from Pc 4 at 675 nm, confirming FRET from the NAO-Pc 4 couple in PC-3 cells.

The observed FRET is biologically plausible because both species reside in mitochondrial regions enriched for CL or Bcl-2/Bcl-xL, which are associated with contact sites. It is also chemically plausible, because both NAO and Pc 4 are large planar aromatic molecules (Fig. 1A) and, thus, have large transition dipole moments, which can interact favorably. FRET is a unique molecular tool to obtain distance information about biological structures in the range of 1–10 nm (18). FRET is the physical process by which energy is transferred nonradiatively from an excited donor molecule (NAO) to a ground state energy acceptor (Pc 4). The essential requirement for effective FRET is that the spectral overlap between the fluorescence of the energy donor (NAO) and the absorbance of the acceptor (Pc 4) are sufficiently strong. This requirement is satisfied for the system under investigation, with a fluorescence quantum yield $\phi_{\text{fl}}(\text{NAO}) = 0.4$ in the absence of Pc 4 and an absorption coefficient $\epsilon_{\text{abs}}(\text{Pc 4}) > 2 \times 10^5 \text{ M}^{-1} \text{ cm}^{-1}$.

This technique should prove valuable for assessing the extent to which other photosensitizers and additional fluorescent drugs bind to mitochondrial sites housing CL. Although some porphyrins are not suitable for such a study because of their strong absorption in the same wavelength range in which NAO absorbs, other Pc, naphthalocya-

nines, and some chlorins and bacteriochlorins might well be investigated in this way. It may also be possible to adapt the procedure for porphyrins by activating NAO at a wavelength at which the porphyrin absorption shows a minimum.

For the NAO-Pc 4 system there are several features that reduce the efficiency of FRET: only a portion of the Pc 4 colocalizes with NAO in mitochondria (Fig. 1B); the concentrations of NAO used are well below saturation of CL sites (11); the emission spectrum of NAO does not overlap well with the absorption spectrum of Pc 4 (Fig. 3A); and the fluorescence quantum yield of Pc 4 was determined to be 7%. Nonetheless, the quantum efficiency of the process is sufficient to produce observable energy transfer that can be used to estimate the distance between NAO and Pc 4.

The decrease in integrated emission intensity of NAO in the presence of Pc 4 was 6.8%. Considering that the fluorescence quantum

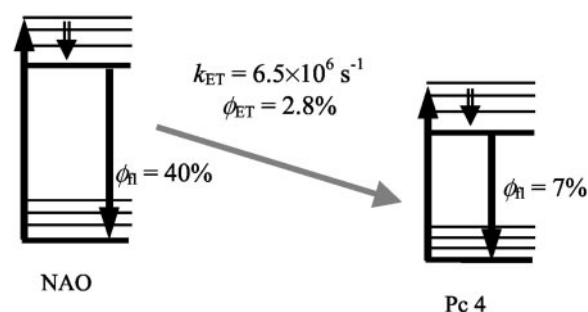


Fig. 4. Schematic to illustrate FRET between NAO and Pc 4.

yield of NAO is 40% leads to a quantum efficiency for the energy transfer of $\phi_{ET} = 2.8\%$ (Fig. 4). Thus, it is not surprising that no measurable decrease was observed by flow cytometry in the 525-nm fluorescence band (Fig. 2A).

The excited state lifetime, τ_{fl} , is related to the radiative rate constant, k_{fl} , and the nonradiative rate constant, k_{nr} , through $\tau_{fl} = (k_{fl} + k_{nr})^{-1}$. The fluorescence quantum yield, ϕ_{fl} , is related to the same parameters through $\phi_{fl} = k_{fl}/(k_{fl} + k_{nr})$. Therefore, knowing the excited state lifetimes and fluorescence quantum yield, k_{fl} and k_{nr} can be calculated directly by equations $k_{fl} = \phi_{fl}/\tau_{fl}$ and $k_{nr} = (1 - \phi_{fl})/\tau_{fl}$. Using tabulated (19) values for acridine orange, $\tau_{fl} = 4.4$ ns and $\phi_{fl} = 40\%$, we can calculate the fluorescence and non-radiative rate of the energy donor NAO to be $k_{fl} = 9 \times 10^7$ s⁻¹ and $k_{nr} = 1.4 \times 10^8$ s⁻¹. This permits determination of the Foerster energy transfer rate (k_{ET}) using $k_{ET} = 1/\tau_{fl} \times 1/(\phi_{fl}^{-1} - 1)$, which results in a $k_{ET} = 6.5 \times 10^6$ s⁻¹ (20). The mechanism of the FRET between NAO and Pc 4 is summarized in Fig. 4.

The information obtained above can be used to derive a distance between the two chromophores, assuming that the donor-acceptor couple has a sufficient degree of rotational freedom, which is generally true for membrane-embedded molecules.

With $k_{ET} = \tau_{fl}^{-1} \times (R_0/R)$ (6), it is possible to estimate the distance between the donor and acceptor in terms of the characteristic Foerster length R_0 , specific for NAO-Pc 4. By calculating the overlap integral $J\lambda$ from the spectroscopic data, the Foerster distance R_0 for the NAO-Pc 4 couple was determined to be 4.02 nm. This gives an intermolecular distance of 7.23 nm for the two chromophores in the biological system, assuming an averaged dipole-dipole arrangement ($\kappa^2 = 2/3$; Ref. 20).

The observed photodamage to Bcl-2 and Bcl-xL by Pc 4-PDT occurs in all of the human cancer cells that have been studied, including PC-3 cells.⁴ Moreover, in preliminary studies of animal tumor models, we found that Pc 4 accumulates in cytoplasmic membranes of the tumor cells and that Bcl-2 of a human tumor xenograft is photodamaged on Pc 4-PDT. Therefore, the location and action of Pc 4 *in vivo* seems to be mimicked by the conditions *in vitro*.

On the basis of the photodamage to Bcl-2 and Bcl-xL, we reasoned that mitochondrial Pc 4 might be localized to the outer membrane, which houses those proteins. The present study suggests that Pc 4 resides near CL-containing sites, which are primarily on the inner mitochondrial membrane. This apparent discrepancy could be resolved if relevant components of the inner membrane (CL) and outer membrane (Bcl-2, Bcl-xL, Pc 4) converge at the contact sites. Alternatively, because some proteins of the contact sites (*e.g.*, voltage-dependent anion channel) are not photodamaged by Pc 4-PDT (5), the effects on Bcl-2 and Bcl-xL may result from those molecules of Pc 4 located elsewhere in the cell, *e.g.*, on the endoplasmic reticulum.

The demonstration of FRET between NAO and Pc 4 indicates that Pc 4 is closely colocalized with CL at its mitochondrial sites and focuses attention on CL as a potential primary target of photodynamically generated singlet oxygen. CL is an attractive candidate for photooxidation because each molecule contains four unsaturated fatty

acids that are easily attacked by singlet oxygen, the cytotoxic mediator of Pc 4-PDT. Nevertheless, future studies are needed to determine whether the binding of Pc 4 to sites near CL causes its oxidation by PDT and whether oxidative damage of CL is necessary for the induction of apoptosis.

Acknowledgments

We thank Dr. Thomas H. Foster (University of Rochester, Rochester, NY) for helpful discussions.

References

- Oleinick, N. L., Morris, R. L., and Belichenko, I. The role of apoptosis in response to photodynamic therapy: what, where, why, and how. *Photochem. Photobiol. Sci.*, *1*: 1–21, 2002.
- Oleinick, N. L., Antunez, A. R., Clay, M. E., Rihter, B. D., and Kenney, M. E. New phthalocyanine photosensitizers for photodynamic therapy. *Photochem. Photobiol.*, *57*: 242–247, 1993.
- Lam, M., Oleinick, N. L., and Nieminen, A. L. Photodynamic therapy-induced apoptosis in epidermoid carcinoma cells. Reactive oxygen species and mitochondrial inner membrane permeabilization. *J. Biol. Chem.*, *276*: 47379–47386, 2001.
- Usuda, J., Chiu, S. M., Murphy, E. S., Lam, M., Nieminen, A. L., and Oleinick, N. L. Domain-dependent photodamage to Bcl-2. A membrane anchorage region is needed to form the target of phthalocyanine photosensitization. *J. Biol. Chem.*, *278*: 2021–2029, 2003.
- Xue, L. Y., Chiu, S. M., and Oleinick, N. L. Photochemical destruction of the Bcl-2 oncoprotein during photodynamic therapy with the phthalocyanine photosensitizer Pc 4. *Oncogene*, *20*: 3420–3427, 2001.
- Moan, J., and Berg, K. The photodegradation of porphyrins in cells can be used to estimate the lifetime of singlet oxygen. *Photochem. Photobiol.*, *53*: 549–553, 1991.
- Tsujimoto, Y., and Shimizu, S. The voltage-dependent anion channel: an essential player in apoptosis. *Biochimie*, *84*: 187–193, 2002.
- Crompton, M., Barksby, E., Johnson, N., and Capano, M. Mitochondrial intermembrane junctional complexes and their involvement in cell death. *Biochimie*, *84*: 143–152, 2002.
- Schlame, M., Rua, D., and Greenberg, M. L. The biosynthesis and functional role of cardiolipin. *Prog. Lipid Res.*, *39*: 257–288, 2000.
- McMillin, J. B., and Dowhan, W. Cardiolipin and apoptosis. *Biochim. Biophys. Acta*, *1585*: 97–107, 2002.
- Petit, J. M., Maftah, A., Ratinaud, M. H., and Julien, R. 10-N-nonyl Acridine orange interacts with cardiolipin and allows the quantification of this phospholipid in isolated mitochondria. *Eur. J. Biochem.*, *209*: 267–273, 1992.
- Jacobson, J., Duchon, M. R., and Heales, S. J. Intracellular distribution of the fluorescent dye nonyl acridine orange responds to the mitochondrial membrane potential: implications for assays of cardiolipin and mitochondrial mass. *J. Neurochem.*, *82*: 224–233, 2002.
- Guidot, D. M. Endotoxin pretreatment *in vivo* increases the mitochondrial respiratory capacity in rat hepatocytes. *Arch. Biochem. Biophys.*, *354*: 9–17, 1998.
- Garcia Fernandez, M., Troiano, L., Moretti, L., Pedrazzi, J., Salvioli, S., Castilla-Cortazar, I., and Cossarizza, A. Changes in intramitochondrial cardiolipin distribution in apoptosis-resistant HCW-2 cells, derived from the human promyelocytic leukemia HL-60. *FEBS Lett.*, *478*: 290–294, 2000.
- Wilson, B. C., Olivo, M., and Singh, G. Subcellular localization of Photofrin and aminolevulinic acid and photodynamic cross-resistance *in vitro* in radiation-induced fibrosarcoma cells sensitive or resistant to Photofrin-mediated photodynamic therapy. *Photochem. Photobiol.*, *65*: 166–176, 1997.
- Ricchelli, F., Nikolov, P., Gobbo, S., Jori, G., Moreno, G., and Salet, C. Interaction of phthalocyanines with lipid membranes: a spectroscopic and functional study on isolated rat liver mitochondria. *Biochim. Biophys. Acta*, *1196*: 165–171, 1994.
- Petit, J. M., Huet, O., Gallet, P. F., Maftah, A., Ratinaud, M. H., and Julien, R. Direct analysis and significance of cardiolipin transverse distribution in mitochondrial inner membranes. *Eur. J. Biochem.*, *220*: 871–879, 1994.
- Stryer, L. Fluorescence energy transfer as a spectroscopic ruler. *Annu. Rev. Biochem.*, *47*: 819–846, 1978.
- Murov, S. L., Carmichael, I., and Hug, G. L. *Handbook of Photochemistry*, pp. 39–40. New York: Marcel Dekker Inc., 1993.
- Clegg, R. M. Fluorescence resonance energy transfer. *Curr. Opin. Biotechnol.*, *6*: 103–110, 1995.